ChemComm

Synthesis of unsymmetrical Si-rhodamine fluorophores and application to a far-red to near-infrared fluorescence probe for hypoxia

Journal:	*ChemComm*
Manuscript ID	CC-COM-03-2018-002451.R1
Article Type:	Communication

ChemComm

COMMUNICATION

Synthesis of unsymmetrical Si-rhodamine fluorophores and application to a far-red to near-infrared fluorescence probe for hypoxia

Received 00th January 20xx,
Accepted 00th January 20xx

DOI: 10.1039/x0xx00000x

Rsc.li/chemcomm

Kenjiro Hanaoka,*[a] Yu Kagami,[a] Wen Piao,[a] Takuya Myochin,[a] Koji Numasawa,[a] Yugo Kuriki,[a] Takayuki Ikeno,[a] Tasuku Ueno,[a] Toru Komatsu,[a] Takuya Terai,[a] Tetsuo Nagano,[b] and Yasuteru Urano *[a,c,d]

Si-rhodamines are bright fluorophores with red to near-infrared (NIR) emission, and are widely used for fluorescence imaging of biological phenomena. Here, in order to extend the scope of Si-rhodamine fluorophores, we established a versatile synthesis of unsymmetrical Si-rhodamines. To illustrate its value, we used one of these new fluorophores to synthesize a far-red to NIR fluorescence probe for hypoxia, and showed that it can visualize hepatic ischemia in mice in vivo.

Fluorescence imaging is one of the most powerful techniques for visualization of biological events in living samples with high temporal and spatial resolution.[1] For fluorescence imaging, activatable fluorescence probes are indispensable and have been extensively investigated.[2] Among them, red to near-infrared (NIR) fluorescence probes are of particular interest for studying biological phenomena inside the body because of the high tissue transparency and low background in this wavelength range, and also because of the potential for multicolour imaging using red-fluorescent probes in combination with widely available green-fluorescent probes to study cellular events at the molecular level.[1,3] We have previously developed Si-rhodamines as practical red-to-NIR fluorophores, and they have found extensive applications, including in vivo imaging, multicolour imaging and super-resolution microscopy.[4,5] Many symmetrical Si-rhodamines have been developed, but so far, very few unsymmetrical Si-rhodamines have been reported, probably due to the lack of suitable synthetic methods.[4,5]

Nevertheless, unsymmetrical rhodamines are expected to be very useful as scaffolds of activatable fluorescence probes, since they would contribute to precise modulation of the absorption and emission wavelengths, as well as the HOMO and LUMO energy levels of the fluorophore, which are deeply related to the fluorescence off/on switching mechanisms of fluorescent probes (e.g. photoinduced electron transfer (PeT),[6] intramolecular spirocyclization,[7] etc.).[8] In addition, it would be possible to introduce two different functionalities into both sides of the xanthene ring of unsymmetrical rhodamine scaffolds.[9] Therefore, we set out to develop a versatile synthetic scheme for unsymmetrical Si-rhodamines.

The established synthetic scheme of symmetrical Si-rhodamines involves homodimerization reaction of two anilines (Scheme 1).[6] Thus, we considered that aniline heterodimers would be key intermediates for the synthesis of unsymmetrical Si-rhodamines. Initially, we tried to synthesize aniline heterodimers by use of the same reaction conditions as

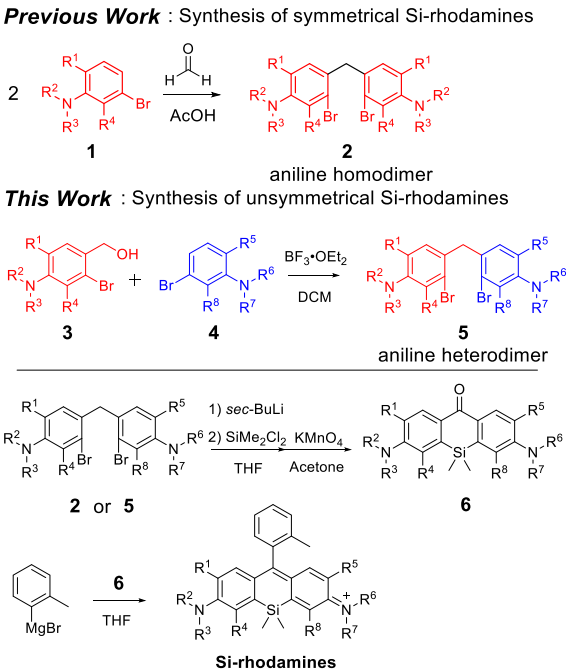

Scheme 1 General synthetic scheme of symmetrical and unsymmetrical Si-rhodamines.

[a] Graduate School of Pharmaceutical Sciences, The University of Tokyo, 7-3-1 Hongo, Bunkyo-ku, Tokyo 113-0033, Japan.
[b] Drug Discovery Initiative, The University of Tokyo, 7-3-1 Hongo, Bunkyo-ku, Tokyo 113-0033, Japan.
[c] Graduate School of Medicine, The University of Tokyo, 7-3-1 Hongo, Bunkyo-ku, Tokyo 113-0033, Japan.
[d] CREST, Japan Agency for Medical Research and Development (AMED), Chiyoda-ku, Tokyo 100-0004, Japan.

† Electronic Supplementary Information (ESI) available: [details of any supplementary information available should be included here]. See DOI: 10.1039/x0xx00000x

Table 1 Heterodimerization reaction of *p*-hydroxymethyl aniline and aniline

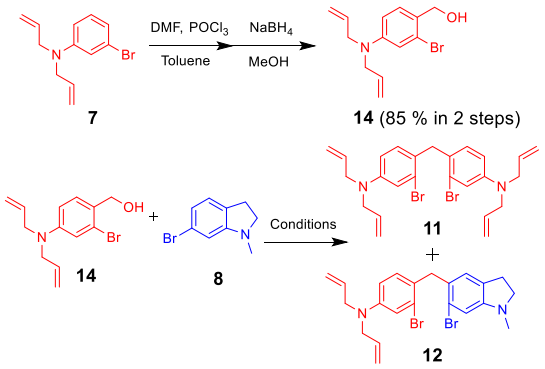

Entry	Conditions	Isolated yield (%) 11	12
1	H_2O/CH_3CN, 80˚C, 48 hr	0	0
2	AcOH, 80˚C, 15 min	67	0
3	$BF_3{\cdot}OEt_2$, DCM, 35˚C, 24 hr	0	65
4	$BF_3{\cdot}OEt_2$, DCM, r.t., 24 hr	0	94

employed for symmetrical Si-rhodamines, but the reaction mainly provided homodimers (see Table S1).

Next, we focused on the Lewis acid-activated nucleophilic substitution reaction of alcohols, and tried to synthesize aniline heterodimers by condensation between aniline and 4-hydroxymethylaniline, which can be activated to the aza quinone methide intermediate by Lewis acid.[10-13] First, a formyl group was introduced into aniline **7** by Vilsmeier reaction, then the formyl group of the product was reduced with $NaBH_4$ to provide *p*-hydroxymethyl aniline (**14**). We then examined the reaction of **14** with aniline **8** under various conditions. We initially tried a mixture of H_2O (proton donor) and CH_3CN as a solvent,[11] but the reaction did not proceed (Table 1, Entry 1). We then examined the conditions used in the previously reported reaction for aniline homodimers, i.e., 80°C for 15 min in acetic acid (Table 1, Entry 2), but this afforded only aniline homodimer **11**, probably because the hydroxy group of **14** was acetylated in this reaction and this product rapidly formed the homodimer **11**.[12] Finally, we used a Lewis acid,[10,13] $BF_3{\cdot}OEt_2$, to efficiently remove the hydroxyl group of **14**. As a result, a moderate yield of aniline heterodimer **12** was obtained in CH_2Cl_2 at 35°C for 24 hrs (Table 1, Entry 3). When the reaction temperature was reduced from 35°C to r.t. in order to prevent side reaction, aniline heterodimer **12** was successfully obtained in high yield (Table 1, Entry 4).

To confirm the usefulness of this synthetic scheme, we synthesized a series of aniline heterodimers (Fig. 1). In the syntheses of **15** and **24**, the temperature was increased to 35°C due to the relatively low reactivity of the anilines (blue anilines in Fig. 1) as nucleophiles. Indeed, when we compared the synthetic yields of **12** (Table 1) and **24**, which are the same compound, the yield was much lower in the latter case, probably because of the relatively low reactivity of 3-bromo-*N*,*N*-diallylaniline as a nucleophile. Among these aniline heterodimers, we selected seven for lithiation with *sec*-BuLi, followed by reaction with $SiMe_2Cl_2$, and then oxidation with $KMnO_4$ to provide Si-xanthones. Reaction of the Si-xanthones with *o*-tolylmagnesium bromide afforded the corresponding unsymmetrical Si-rhodamines (Scheme 1). These Si-rhodamines

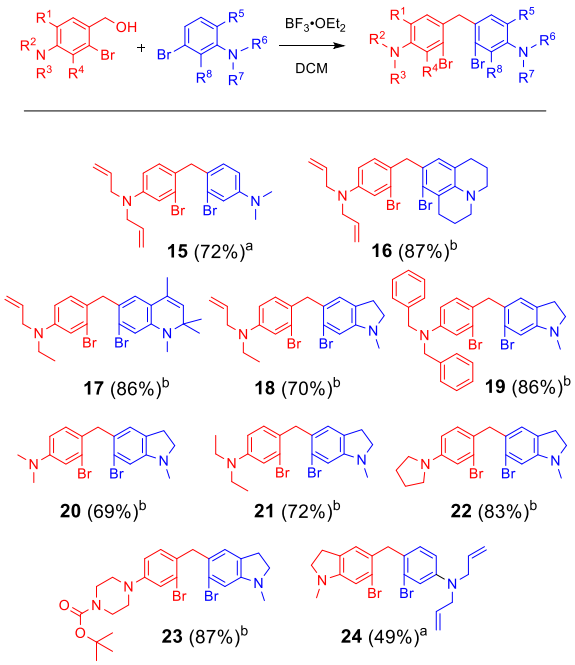

Fig. 1 Synthesized aniline heterodimers. The isolated yields are shown in parentheses. The reactions were performed at (a) 35°C or (b) r.t.

showed various absorption and emission wavelengths from 620 nm to 700 nm with relatively high fluorescence quantum yields (Fig. 2 and Fig. 3). Fluorophores **25** and **28** are of particular interest as their absorption and emission wavelengths are intermediate between those of symmetrical Si-rhodamines, 2-Me SiR600, 2-Me SiR650 and 2-Me SiR700,[14] as are their LUMO energy levels, which are important for the PeT and intramolecular spirocyclization mechanisms (Fig. S1, Fig. S2). We calculated the HOMO and LUMO energy levels of these seven unsymmetrical Si-rhodamines and three previously reported symmetrical Si-rhodamines at the B3LYP/6-31+G(d) (gas phase) level, and found that the differences between the HOMO and LUMO energy levels of the fluorophores, except **31**, were highly correlated with their absorption wavelengths (Fig. S3). The exception in the case of **31** is probably due to the extension of the π conjugation system. This result indicates that absorption wavelengths of Si-rhodamines can be predicted from the calculated HOMO and LUMO energy levels before synthesis, which would be helpful to obtain fluorophores optimized for the absorption and emission wavelengths of existing microscope lasers and emission filters.

Finally, to demonstrate the usefulness of unsymmetrical Si-rhodamines for the development of novel far-red to NIR fluorescence probes, we designed and synthesized a NIR fluorescence probe for hypoxia, which is associated with various diseases.[15] In some solid tumours, the median oxygen concentration has been reported to be around 4% and locally it may even fall to 0%.[16]

The hypoxia has various biological consequences, including stabilization of hypoxia-inducible factor 1α (HIF-1α) and modulation of HIF-mediated gene expression.[17] We have previously developed azo rhodamine derivatives, MAR and MASR, as hypoxia-sensitive fluorescence probes and demonstrated that MAR could visualize retinal hypoxia in a rat artery occlusion model.[18] However, from the viewpoint of in vivo imaging, it would be useful to extend the range

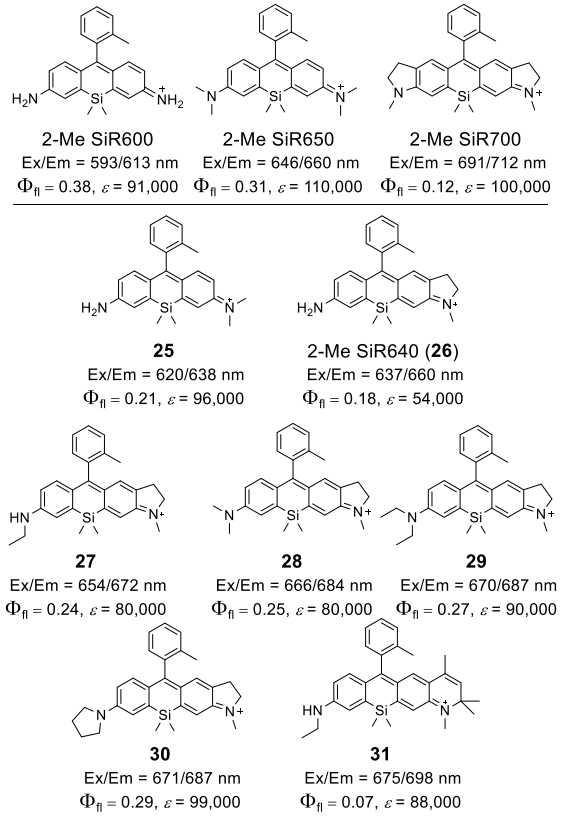

Fig. 2 Synthesized unsymmetrical Si-rhodamines and their photophysical properties in 100 mM sodium phosphate buffer (pH 7.4) containing 1% DMSO as a co-solvent. Symmetrical Si-rhodamines, 2-Me SiR600, 2-Me SiR650 and 2-Me SiR700, were previously reported.[14] Φ_{fl}: fluorescence quantum yield. ε: molar extinction coefficient.

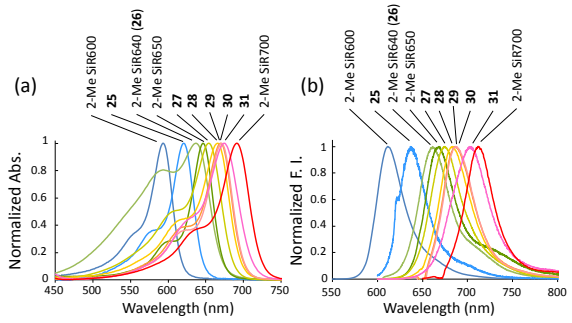

Fig. 3 (a,b) Normalized absorption (a) and emission (b) spectra of reported symmetrical Si-rhodamines (2-Me SiR600, 2-Me SiR650 and 2-Me SiR700) and unsymmetrical Si-rhodamines **25**-**31**. Absorption and emission spectra were measured in 100 mM sodium phosphate buffer (pH 7.4) containing 1% DMSO co-solvent.

of available excitation and emission wavelengths to achieve deep tissue penetration and low scattering. For this purpose, we focused on SiR640 (**26**) as a scaffold fluorophore, because SiR640 shows NIR emission and has an amino group on the xanthene moiety (Fig. 2 and Fig. 3) and this group can be structurally modified to obtain a suitable functional moiety for fluorescence off/on switching. The designed probe, azoSiR640 (Fig. 4a), was easily synthesized by azo coupling reaction with 2,6-diMe SiR640 (see Supporting Information).

azoSiR640 showed a broad absorbance spectrum with no fluorescence in PBS (Fig. S4, Table S2). A 2,6-dimethylbenzene moiety was included in the probe structure to prevent nucleophilic attack of water molecules and/or reduced glutathione (GSH) on the 9-position of the Si-xanthene moiety of azoSiR640.[19] To confirm the stability of azoSiR640, we examined the reactivity of azoSiR640 with 0-10 mM GSH, and found that azoSiR640 was stable even in the presence of 10 mM GSH (Fig. S4). In the assay of azoSiR640 with rat liver microsomes, which contain various bioreductases, a large fluorescence increase was observed only under hypoxia and the fluorescence intensity was increased 43-fold compared with that under normoxia (Fig. 4b). A small fluorescence decrease was observed under hypoxia after the maximum fluorescence intensity was reached, probably due to reduction of the fluorophore, 2,6-diMe SiR640. However, this phenomenon is not problematic for fluorescence imaging of hypoxia, because no significant fluorescence decrease of 2,6-diMe SiR640 was observed in living cells under hypoxia (Fig. S5). HPLC analyses of reaction mixtures of azoSiR640 with rat liver microsomes also revealed that 2,6-diMe SiR640 was generated only under hypoxia (Fig. S6).

To examine whether or not this fluorescence probe can detect hypoxia in living cells, A549 cells were incubated with 100 nM azoSiR640 under various oxygen concentrations for 6 hr and fluorescence imaging was performed. A significant fluorescence increase was observed at 5% oxygen concentration and below (Fig. 4c,d). This fluorescence increase was diminished in a concentration-dependent manner by the non-specific flavoprotein inhibitor diphenyliodonium chloride (DPI) (Fig. S7). This result suggests that the probe is reduced by flavoproteins, including NADPH-cytochorome P450 reductase, which are thought to be responsible for the metabolic activation of bioreductive compounds under hypoxia.[20] We also successfully performed real-time live-cell imaging of hypoxia by placing a cover glass over a cell monolayer[18,21] (Fig. S8, Supplementary movie 1).

Finally, we conducted fluorescence imaging in mice to detect hypoxia in vivo. AzoSiR640 was administered through an orbital vein, and then the portal and renal veins were ligated to induce liver and kidney ischemia. Time-lapse in-vivo NIR fluorescence imaging was performed (Fig. 4e). Before ligation of the portal and renal veins, no fluorescence increase was observed at the liver and kidney. On the other hand, after ligation, strong fluorescence was observed at both liver and kidney, with increases of 10-fold and 3-fold after 20 minutes, respectively (Fig. S9, Supplementary movie 2). On the other hand, there was no fluorescence increase in the small intestine, which was not ligated.

In summary, we have established a novel synthetic strategy for unsymmetrical Si-rhodamines via aniline heterodimers. These unsymmetrical Si-rhodamine fluorophores provide new opportunities for modulating absorption and emission wavelengths, as well as HOMO and LUMO energy levels, which are important for fluorescence off/on switching.[22] To illustrate their utility, we employed the newly synthesized unsymmetrical Si-rhodamine, 2,6-diMe SiR640, to develop a far-red to NIR fluorescence probe for hypoxia, azoSiR640. We also found that the calculated HOMO and LUMO energy levels of Si-rhodamines can be useful to predict the absorption wavelengths and the HOMO and LUMO energy levels of fluorophores, which are important determinants of the fluorescence

off/on switching properties.[23] We believe that the synthetic availability of unsymmetrical Si-rhodamines opens up new opportunities for expanding the range of applications of red-to-NIR fluorescence probes.

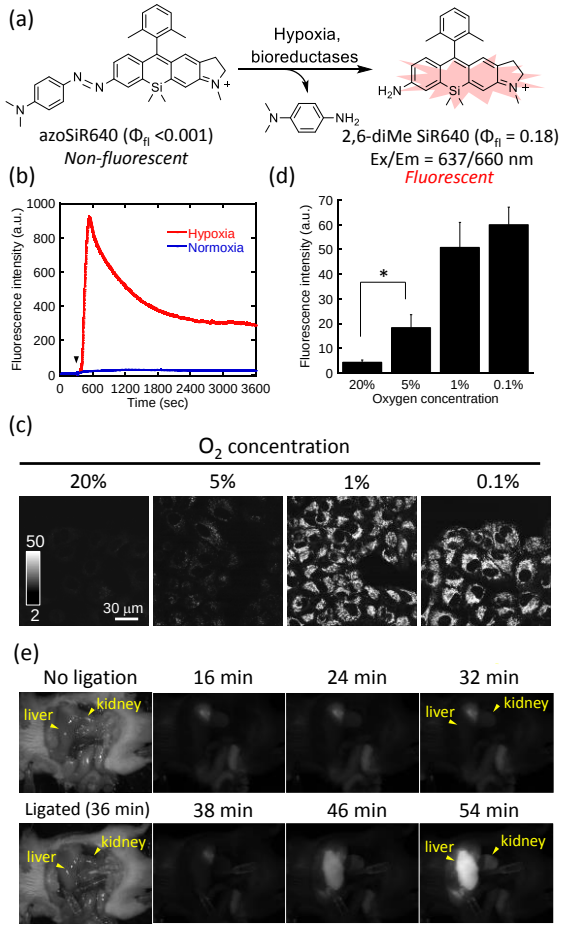

Fig. 4 Far-red to NIR fluorescence probe for hypoxia, azoSiR640. (a) NIR fluorescence activation of azoSiR640. azoSiR640 is almost non-fluorescent, but is reduced by bioreductases under hypoxia to strongly fluorescent 2,6-diMe SiR640. (b) Time-dependent changes in the fluorescence intensity of azoSiR640 (1 μM) in the presence of rat liver microsomes (226 μg/3 mL) under hypoxia or normoxia. Measurements were performed in a potassium phosphate buffer (0.1 M; pH 7.4) containing DMSO (0.1%) as a cosolvent. As a cofactor for reductases, NADPH (50 μM) was added after 5 min (arrowhead). The excitation and emission wavelengths were 640 and 660 nm. (c) Fluorescence confocal microscopy images of live A549 cells. A549 cells were incubated with azoSiR640 (100 nM) containing DMSO (0.1%) as a cosolvent at various oxygen concentrations for 6 hr. (d) Quantitation of fluorescence intensity at ROI of cells under various oxygen concentrations. n = 4. * indicates p<0.05 by Student's t-test. (e) Fluorescence images of mouse. ICR mouse was injected with 100 μM azoSiR640 in 100 μL saline solution containing 1% DMSO as a cosolvent from an orbital vein. The portal vein and renal vein were ligated about 35 min after probe injection. Excitation and emission wavelengths were 635 nm and 700 nm, respectively. Exposure time: 300 ms.

This work was supported in part by grants by JSPS KAKENHI Grant Numbers 16H00823, 16H05099 and 18H04609 to K.H., and SENTAN, JST to K.H., who was also supported by Mochida Memorial Foundation for Medical and Pharmaceutical Research.

Conflicts of interest

There are no conflicts to declare.

Notes and references

1 B. N. G. Giepmans, S. R. Adams, M. H. Ellisman and R. Y. Tsien, *Science*, 2006, **312**, 217-224.
2 T. Ueno and T. Nagano, *Nat. Methods*, 2011, **8**, 642-645.
3 R. Weissleder and V. Ntziachristos, *Nat. Med.*, 2003, **9**, 123-128.
4 Y. Kushida, T. Nagano and K. Hanaoka, *Analyst*, 2015, **140**, 685-695.
5 T. Ikeno, T. Nagano and K. Hanaoka, *Chem. Asian J.*, 2017, **12**, 1435-1446.
6 Y. Koide, Y. Urano, K. Hanaoka, T. Terai and T. Nagano, *ACS Chem. Biol.*, 2011, **6**, 600-608.
7 S. Uno, M. Kamiya, T. Yoshihara, K. Sugawara, K. Okabe, M. C. Tarhan, H. Fujita, T. Funatsu, Y. Okada, S. Tobita and Y. Urano, *Nat. Chem.*, 2014, **6**, 681-689.
8 H. Sasaki, K. Hanaoka, Y. Urano, T. Terai and T. Nagano, *Bioorg. Med. Chem.*, 2011, **19**, 1072-1078.
9 J. Lee, K. H. Lee, J. Jeon, A. Dragulescu-Andrasi, F. Xiao and J. Rao, *ACS Chem. Biol.*, 2010, **5**, 1065-1074.
10 C. Y. Tsai, R. Sung, B. R. Zhuang and K. Sung, *Tetrahedron*, 2010, **66**, 6869-6872.
11 H. Takahashi, N. Kashiwa, H. Kobayashi, Y. Hashimoto and K. Nagasawa, *Tetrahedron Lett.*, 2002, **43**, 5751-5753.
12 Y. Y. Lai, N. T. Lin, Y. H. Liu, Y. Wang and T. Y. Luh, *Tetrahedron*, 2007, **63**, 6051-6055.
13 K. Kolmakov, V. N. Belov, C. A. Wurm, B. Harke, M. Leutenegger, C. Eggeling and S. W. Hell, *Eur. J. Org. Chem.*, 2010, 3593-3610.
14 (a) Y. Koide, Y. Urano, K. Hanaoka, W. Piao, M. Kusakabe, N. Saito, T. Terai, T. Okabe and T. Nagano, *J. Am. Chem. Soc.*, 2012, **134**, 5029-5031; (b) Y. Kushida, K. Hanaoka, T. Komatsu, T. Terai, T. Ueno, K. Yoshida, M. Uchiyama and T. Nagano, *Bioorg. Med. Chem. Lett.*, 2012, **22**, 3908-3911.
15 G. L. Semenza, *N. Engl. J. Med.*, 2011, **365**, 537-547.
16 P. Vaupel, K. Schlenger, C. Knoop and M. Höckel, *Cancer Res.*, 1991, **51**, 3316-3322.
17 U. Lendahl, K. L. Lee, H. Yang and L. Poellinger, *Nat. Rev. Genet.*, 2009, **10**, 821-832.
18 W. Piao, S. Tsuda, Y. Tanaka, S. Maeda, F. Liu, S. Takahashi, Y. Kushida, T. Komatsu, T. Ueno, T. Terai, T. Nakazawa, M. Uchiyama, K. Morokuma, T. Nagano and K. Hanaoka, *Angew. Chem. Int. Ed.*, 2013, **52**, 13028-13032.
19 T. Myochin, K. Hanaoka, S. Iwaki, T. Ueno, T. Komatsu, T. Terai, T. Nagano and Y. Urano, *J. Am. Chem. Soc.*, 2015**, 137**, 4759-4765.
20 W. R. Wilson and M. P. Hay, *Nat. Rev. Cancer* 2011, **11**, 393-410.
21 E. Takahashi and M. Sato, *Am. J. Cell Physiol.*, 2010, **299**, C1318-C1323.
22 S. Takahashi, Y. Kagami, K. Hanaoka, T. Terai, T. Komatsu, T. Ueno, M. Uchiyama, I. Koyama-Honda, N. Mizushima, T. Taguchi, H. Arai, T. Nagano and Y. Urano, *J. Am. Chem. Soc.*, 2018, **140**, 5925-5933.
23 R. J. Iwatate, M. Kamiya, K. Umezawa, H. Kashima, M. Nakadate, R. Kojima and Y. Urano, *Bioconjugate Chem.*, 2018, **29**, 241-244.

Graphical Abstract

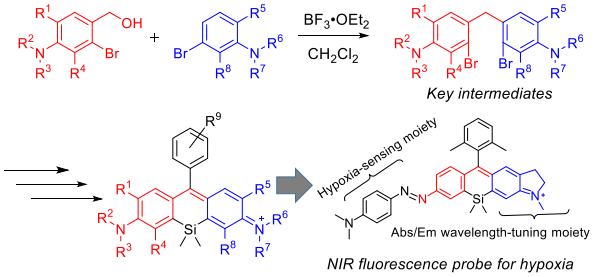

A versatile synthesis of unsymmetrical Si-rhodamines was established and applied for development of a hypoxia-sensing far-red to NIR fluorescence probe.